RSC Advances

PAPER

Cite this: *RSC Adv.*, 2015, **5**, 6758

Influence of the degree of polymerisation and of the architecture on the elastic properties of new polyurea elastomers†

Antoni Sánchez-Ferrer,‡*[a] Daniel Rogez[b] and Philippe Martinoty*[b]

The elastic properties of new polyurea elastomers have been studied by varying the segmental molecular weight and the chemical nature of the polymer end groups. Three different types of elastomers were synthesized leading to three different types of response. The elastomers with a high degree of polymerisation and primary amines as terminal groups show two plateaus: at high temperature, the common permanent plateau related to the rubber behaviour of elastomeric systems and, at low temperature, a transient plateau associated with the hydrogen bonding of the urea motives occurring in the interfacial zone between the soft polyetheramine and the hard crosslinker domains. The elastomers with a low degree of polymerization and primary amines as terminal groups show that the transient plateau is masked by the glassy plateau because the hydrogen bonds occur in the same temperature range as the glass transition effects, except for very slow heating rates for which the transient network can be resolved. Lastly, the elastomers with no hydrogen bonding just show the common step in the elastic behaviour from the rubbery to the glassy state.

Received 5th September 2014
Accepted 17th December 2014

DOI: 10.1039/c4ra09879j

www.rsc.org/advances

Introduction

Polyurethane, polyurethane/polyurea, and polyurea materials can be found in several day-to-day applications in the medical field,[1–4] *i.e.*, cardiovascular applications, reconstructive surgery, gynaecology and obstetrics, organ regeneration in tissue engineering, and medical supplies, which can be formed by machine moulding, liquid moulding and fibre spinning for tubing, coatings, foams, fibres, sheets and film production.[5]

Polyurea chemistry is based on a chemical reaction between the electrophilic isocyanate group and the nucleophilic amine group to form urea motives which establish hydrogen bonds. Polyurea elastomers are very attractive materials due to their enhanced mechanical properties and their chemical resistance when compared to polyurethanes. Unlike the latter, the fast reaction between isocyanates and amines does not require a catalyst.[6,7] Moreover, the chemical structure and molecular weight of both the phase-separated soft (amino compound) and hard (isocyanate compound) domains, as well as the stoichiometric ratio, control the final mechanical and chemical properties of the engineered polyurea material. When chemically crosslinked, polyurea elastomers combine the mechanical properties of chemical (covalent bonds) and physical (hydrogen bonds) networks in one single material.[8–11]

The reaction between a diamino- or triamino-terminated polymer melt and a polyisocyanate leads to polyurea elastomers characterized by both soft domains coming from the low glass transition temperature segment of the amino-functionalised polymer, and hard domains from the polyisocyanate core and urea motives appearing during the reaction.[12] These urea groups have the ability of establishing hydrogen bonds in a mono- or bidentated fashion[13,14] which act both as fillers and physical crosslinking sites. The corresponding reinforcement of the polymer network due to these hydrogen bonds grants polyurea systems the ability to act as high performance polymers with better mechanical and chemical resistance, flexibility, toughness, excellent electrical insulating, and good adhesion properties than standard polyurethanes.[15–21]

Numerous experiments were performed to study the behaviour of the complex shear modulus at different temperatures and frequencies. For example, dynamic mechanical analysis (DMA) experiments were carried out on a huge variety of polyurethane[22–25] and polyurea[26–32] elastomers, which are characterized by a glassy plateau stemming from the soft domains followed, when the temperature is increased, by a short rubbery

[a]*Institute of Supramolecular Science and Engineering, University Louis Pasteur, 8 allée Gaspard Monge, Strasbourg, F-67083, France. E-mail: a.sanchez-ferrer@isis.u-strasbg.fr*

[b]*Institute Charles Sadron, UPR 22 CNRS, 23 rue du Loess, Strasbourg Cedex, F-67034, France. E-mail: philippe.martinoty@ics-cnrs.unistra.fr*

† Electronic supplementary information (ESI) available: Chemical structures of the polymer backbones and the corresponding segmental molecular weight, temperature dependent FTIR experiments, DSC thermograms, stress–strain measurements. See DOI: 10.1039/c4ra09879j

‡ Present address: Department of Health Sciences and Technology, ETH Zurich, Schmelzbergstrasse 9, CH-8092, Zurich, Switzerland. E-mail: antoni.sanchez@hest.ethz.ch.

plateau and, at high temperatures, by a zero value of the storage modulus resulting from the melting of the hard semicrystalline domains. As we have shown previously, this melting/flowing at high temperatures could be avoided by imposing chemical crosslinks leading to a second rubbery plateau, which can be observed when introducing urea motives instead of urethane groups.[8–11]

In this paper, the elastic properties of this new kind of polyurea elastomer, obtained *via* sol–gel chemistry,[8] are investigated by systematically changing the degree of polymerisation and architecture of the polymer backbone between crosslinking points, as well as the capability of hydrogen bonding between the urea motives for primary and secondary amines. The measurements of the complex shear modulus $G^* = G' + iG''$ were performed as a function of frequency and temperature with a piezoelectric rheometer. In addition, complementary experiments, namely differential scanning calorimetry (DSC) for the detection of the phase transitions, Fourier-transform infrared (FTIR) spectroscopy for the identification of the hydrogen bonding between the urea motives and stress–strain experiments for the evaluation of the Young's modulus, were also used to characterize these new elastomers.

Experimental part

Materials

The three linear diamino-terminated polyetheramines Jeffamine® D-400 (M_n = 460 Da, DP ≈ 6), D-2000 (M_n = 2060 Da, DP ≈ 34) and D-4000 (M_n = 4000 Da, DP ≈ 68), the three star-like triamino-terminated polyetheramines Jeffamine® T-403 (M_n = 486 Da, DP ≈ 6), T-3000 (M_n = 3180 Da, DP ≈ 50) and T-5000 (M_n = 5712 Da, DP ≈ 85), the two secondary amino-terminated polyetheramines Jeffamine® SD-2001 (M_n = 2050 Da, DP ≈ 33) and ST-404 (M_n = 565 Da, DP ≈ 6) were supplied by Huntsman International LLC. The triisocyanate crosslinker Basonat® HI-100 (M_n = 505 Da) was provided by BASF SE. All chemicals were used as received. Acetone (Aldrich) was used without further purification for the crosslinking of the polyetheramines. The chemical structures for all polyetheramines and the crosslinker are shown in the ESI (Fig. ESI-1†).

Preparation of the polyurea elastomers

The typical procedure to obtain networks with 15% (w/v) of solid content is described in the literature,[8–11] giving as an example the synthesis of the elastomer ED-2000. In two separate 30 mL flasks, the polyetheramine (3.850 g in 8.78 g of acetone) and the crosslinker (0.651 g in 11.41 g of acetone) were dissolved. After 2 h with occasional shaking of the solutions, the contents of the two flasks were mixed and ready to put in a glass capsule. The cast sample was ambient dried after 24 h of reaction at room temperature to make sure that a good crosslinking process took place.

Techniques

Differential scanning calorimetry (DSC) experiments were carried out on a Netzsch DSC 200 F3 Maia apparatus with heating and cooling-rates of 5, 10 and 20 K min^{-1} under nitrogen atmosphere, using 20 μL aluminium pans with holes. The first heating run was use to remove all effects due to thermal history of the elastomer and only second, third and fourth heating and cooling runs were used at different rates on the same piece of elastomer.

Fourier-transform infrared (FTIR) spectra of elastomers were obtained by using a Bruker Tensor 27 FTIR spectrometer equipped with a diamond MKII Golden Gate single attenuated total reflection (ATR) system. Elastomers were scanned over the range of 4000 to 600 cm^{-1} with a resolution of 2 cm^{-1} and averaged over 64 scans.

Stress–strain experiments were performed with a self-constructed apparatus. In a cell controlled by a Haake-F6 thermostat and equipped with a Pt100 thermoresistor, the elastomer was stretched by one Owis SM400 microstep motor and controlled by an Owis SMK01 microstep controller. The stress was measured by a HBM PW4FC3 transducer load cell (300 g) and analysed by an HBMKW3073 high-performance strain gage indicator. All relevant data such as temperature, uniaxial strain ratio ($\lambda = L/L_0$, where L and L_0 are the lengths of the film in the stretched and unstretched states) and uniaxial stress (σ) were continuously logged. A personal computer controlled the deformation stepwise as specified by a script file. After each deformation step, the uniaxial stress was determined at equilibrium (determined by the slope and the standard deviation of the continuously logged data).

The measurements of the complex shear modulus G^* were performed with the piezoelectric rheometer which has been developed over more a decade for studying the rheological properties of several types of materials of soft matter: liquid-crystalline elastomers,[33–42] liquid crystal and conventional polymers,[43–46] uniaxial magnetic gels,[47] suspension of magnetic particles,[48] and polyelectrolyte films.[49] This device is a plate–plate rheometer operating with piezoelectric ceramics vibrating in the shear mode. The principle of measurements is shown in Fig. 1. A very small strain ε is applied on to the sample through the glass slide attached to the emitting ceramic, and the stress σ received on the opposite glass slide is measured by the receiving ceramic attached to this glass slide. The complex shear modulus G^* is given by the stress–strain relationship $G^* = \sigma/\varepsilon$.

The measuring cell is placed in an oven with a temperature controlled to within a tenth of a degree Celsius. The device can

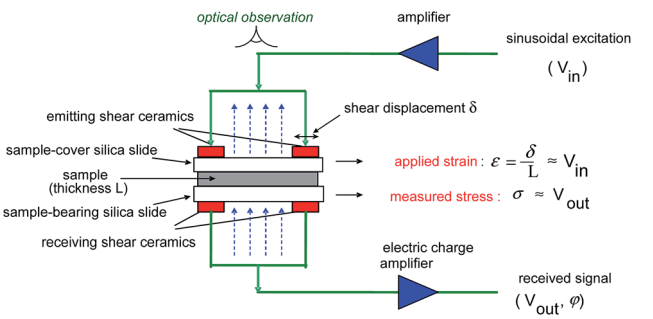

Fig. 1 Block diagram of the piezoelectric rheometer.

acquire data in a very wide frequency range from $f = 2 \times 10^{-2}$ to 10^4 Hz, by imposing very low strains, from $\varepsilon = 10^{-6}$ to 10^{-2}, to samples whose thickness, L, can vary from about ten micrometers (liquid) to a few centimetres (soft solid). The amount of sample required to perform measurements is very small and constitutes another advantage of this device. The temperature range studied can vary from $T = -60$ to +150 °C.

In the present study, the various samples were first heated up to 100 °C outside the piezoelectric rheometer cell, and then placed in the piezoelectric rheometer cell at room temperature. The cell was heated to high temperature (∼+100 °C), and the measurements were taken in a wide temperature range, first by decreasing the temperature down to a low temperature (∼−50 °C), and then by increasing the temperature up to the initial temperature. The cooling and heating rates between two temperatures where the data were taken were 1 h (3 K h^{-1}), and the time required for taking a frequency spectrum at each temperature of measurement was 1 h. Slower ($dT/dt = 1.5$ K h^{-1}) and faster ($dT/dt = 18$ K h^{-1}) cooling/heating rates were also used for one elastomer (ED-400). G^* was determined for frequencies ranging from $f = 0.2$ up to 10^4 Hz. The applied strain was very small $\varepsilon \sim 10^{-4}$, and the validity of the linear response checked experimentally. A PC monitoring the measuring system allowed the measurements to be carried out automatically. The samples were films with thickness around 300 μm and a surface area A around 1 cm^2. To be certain that the mechanical response was not affected by the thickness of the film, samples with higher thickness (750 μm for EST-404 and 1000 μm for ED-400) were also studied.

Results and discussion

Mechanical and thermodynamic behaviour of the elastomers containing diamino-terminated polyetheramines as a function of temperature

A series of four polyurea elastomers containing diamino-terminated polyetheramine (linear polymer) was synthesized by varying the molecular weight of the polymers belonging to the soft domain and the degree of substitution of the amine group. This series includes three samples with primary amino groups ED-400, ED-2000 and ED-4000, which lead to disubstituted urea motives, and one sample with secondary amino groups ESD-2001, which led to trisubstituted urea motives. This choice was done in order to monitor the effect induced by the degree of polymerisation of the polyetheramine as well as the ability to form hydrogen bonds as function of the degree of substitution in the urea motive.

Fig. 2 shows the temperature dependence of G', at the frequency of 1 Hz, for the elastomer ED-2000. At high temperatures, the behaviour of G' is that of a conventional elastomer ($G' \sim k_B T$, where k_B is the Boltzmann constant). As we will see later in the section dealing with the behaviour of the elastomers as a function of frequency, G' is frequency independent and $G'' \propto f$; for the frequencies below ∼300 Hz. This frequency behavior is the one expected for the mechanical response of an elastomer in the hydrodynamic regime. The material is therefore chemically crosslinked at high temperature, which

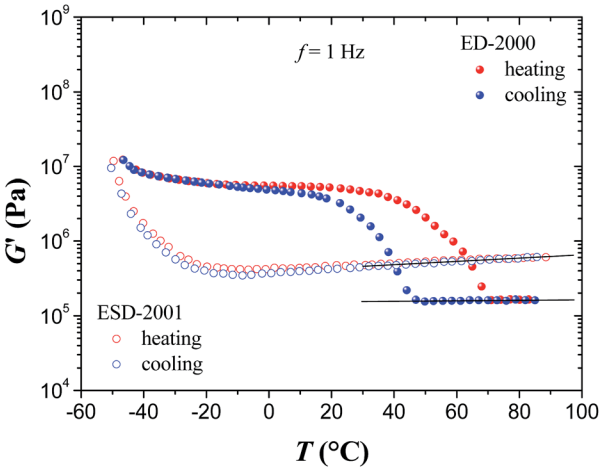

Fig. 2 Comparison between the temperature dependence at $f = 1$ Hz of G' for the elastomer ED-2000 (primary amino-terminated polyetheramine which reacts forming disubstituted urea groups with bidentated hydrogen bonds) and the elastomer ESD-2001 (secondary amino-terminated polyetheramine which reacts forming trisubstituted urea groups without bidentated hydrogen bonds) both at $dT/dt = 3$ K h^{-1}. The data for the elastomer ED-2000 show the presence of a transient network associated with the formation and breaking of hydrogen bonds. The solid lines represent the classical $k_B T$ behaviour.

supports our previous statement indicating that the temperature dependence of G' in the high temperature range is that of a conventional elastomer. By decreasing the temperature, a strong increase in G' of about two orders of magnitude is observed between $T \sim +45$ and 0 °C. Given that the FTIR measurements have revealed the presence of hydrogen bonds in this temperature range,[8] and no sign of crystallinity was observed from X-ray experiments in the wide-angle region proving the amorphous nature of the samples,[8] the mechanical reinforcement of the elastomer can be attributed to a transient network formed by these hydrogen bonds. By increasing the temperature, the data of Fig. 2 show that the mechanical reinforcement disappears at $T \sim +70$ °C. This temperature can therefore be considered as the melting temperature of the transient network formed by the hydrogen bonds. This melting temperature is clearly much higher than the temperature of formation. The large difference between the two temperatures comes from the fact that the hydrogen bonds formation is more difficult to achieve than their breaking. Indeed, upon cooling, the molecules must find each other in order to form the clusters that are at the origin of the network. This effect does not exist in the heating process, leading thus to the large hysteresis observed between the heating and cooling processes.

In order to definitely ascertain that the transient network is caused by the presence of hydrogen bonds, the elastomer ESD-2001, which exhibits no hydrogen bonds, was studied. The temperature dependence of G' is also plotted in Fig. 2 to allow for a direct comparison with the behaviour observed for the elastomer ED-2000. The results show that the strong increase in G' observed by cooling the temperature between $T \sim +45$ and 0 °C has disappeared and is replaced by the classical $k_B T$ behaviour. This result confirms that the transient network of

the elastomer ED-2000 comes from the formation of hydrogen bonds. The data also show that the value associated with the k_BT contribution is higher than that of the elastomer ED-2000, which could be due to the difference in the architecture or in the crosslinking density during sample preparation between the two elastomers. Finally, the strong increase in G' that occurs below $T \sim -20$ °C reflects the influence of the glass transition that is located around $T_g \sim -65$ °C. This influence of the glass transition could also be observed on the G' behaviour of the elastomer ED-2000.[50–52]

Furthermore, elastomers containing both a lower (ED-400) and a higher (ED-4000) molecular weight diamino-terminated polyetheramine polymer (as compared to ED-2000) were also studied. Fig. 3a shows that the behaviour observed for the elastomer ED-4000 is similar to that for the elastomer ED-2000, demonstrating that the response of the elastomer results from the contribution of two components: the classical one (chemical) occurring at high temperature, and a transient one (physical) associated with the formation and the breaking of hydrogen bonds occurring at low temperature. The results obtained for the elastomer ED-400 are shown on Fig. 3b at slow ($dT/dt = 1.5$ K h^{-1}) and fast ($dT/dt = 18$ K h^{-1}) cooling/heating rates. It can be seen that the cooling curve is independent of the small or high value of the cooling rate and does not reveal the presence of the transient network. In contrast, the heating curves depend on the heating rate, and the plateau associated with the transient network is revealed only by the slow heating rate. These observations indicate that short polymers have reduced mobility when crosslinked, which firstly increases the T_g value, and secondly reduces the time for the reformation of any interaction between the urea motives.

The same conclusion is supported by the stress–strain experiments performed at 25 °C on the pristine elastomer and after annealing the sample at 100 °C (Fig. 4). It can be seen that the Young modulus of the elastomer ED-400 after annealing ($E_{100\rightarrow25} = 3.58 \times 10^6$ Pa) is smaller than that of the pristine elastomer ($E_{25} = 2.55 \times 10^7$ Pa). This difference in the thermal history of the sample shows that the annealed elastomer becomes softer due to the removal of the hydrogen bonds which cannot be reformed during the time scale of the experiment (*i.e.*, the time for annealing and for heating and decreasing the temperature, which is typically less than 1 h). This is consistent with the G' values obtained at low cooling rate ($G' \sim 10^6$ Pa) and at low heating rate ($G' \sim 10^7$ Pa). DSC experiments at $dT/dt = 10$ K min^{-1} also showed the removal of the hydrogen bonds upon heating the elastomer ED-400, which only reappeared after leaving the elastomer for long time at room temperature. Fig. 5 shows that the first scan on the elastomer ED-400 reveals the presence of hydrogen bonds by the two peaks at $T_{HB} \sim 64$ and 81 °C ($\Delta H_{HB} \sim 5.2$ J g^{-1}), but after cooling down the sample, the second and posterior heating curves do not show any signal of hydrogen bonds indicating that at this time scale the urea motives could not find each other. After one day at 25 °C, the first heating scan shows one peak at $T_{HB} \sim 68$ °C with 25% of the initial enthalpy ($\Delta H_{HB} \sim 1.3$ J g^{-1}), and only after three weeks the two peaks emerge again at $T_{HB} \sim 68$ and 76 °C recovering 60% of the initial energy ($\Delta H_{HB} \sim 3.2$ J g^{-1}). In

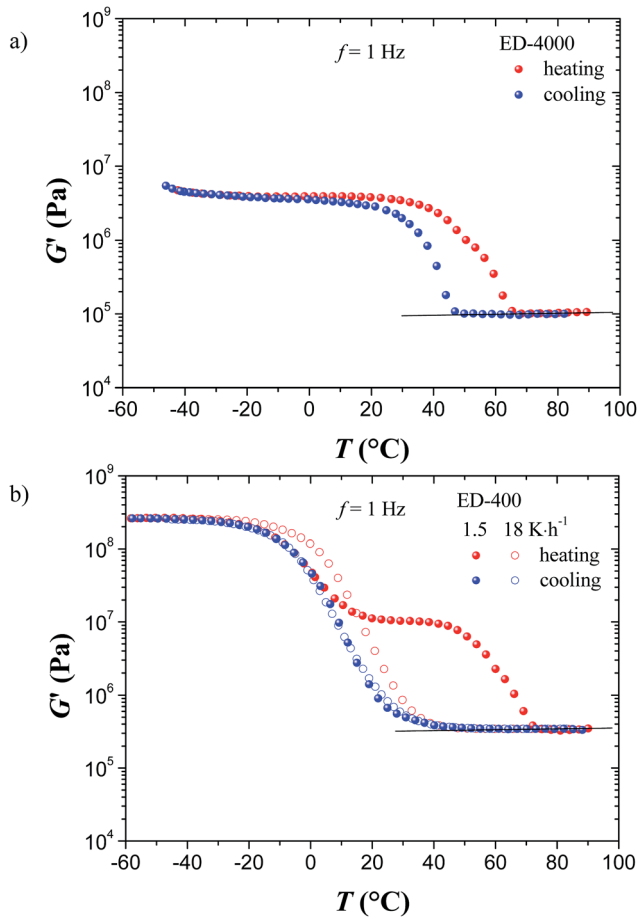

Fig. 3 Temperature dependence at $f = 1$ Hz of G' for (a) the elastomer ED-4000 (long primary amino-terminated polyetheramine) at $dT/dt = 3$ K h^{-1}, and for (b) the elastomer ED-400 (short primary amino-terminated polyetheramine) at $dT/dt = 1.5$ and 18 K h^{-1}. The solid lines represent the classical k_BT behaviour.

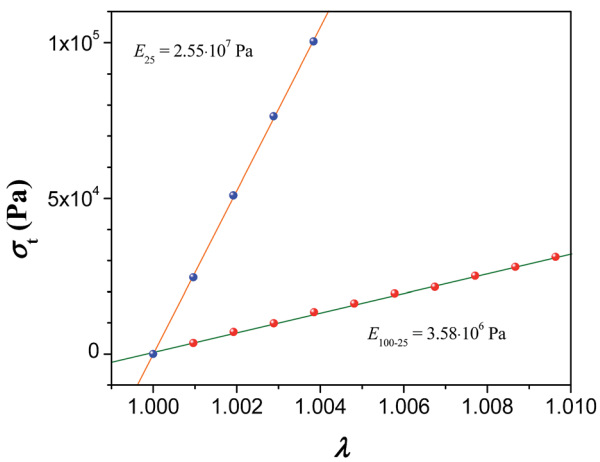

Fig. 4 Stress–strain curves for the elastomers ED-400 at $T = 25$ °C after annealing the sample at 100 °C (●) and directly measured from the synthesis (●). The solid straight lines are the fits of the data belonging to the purely elastic region.

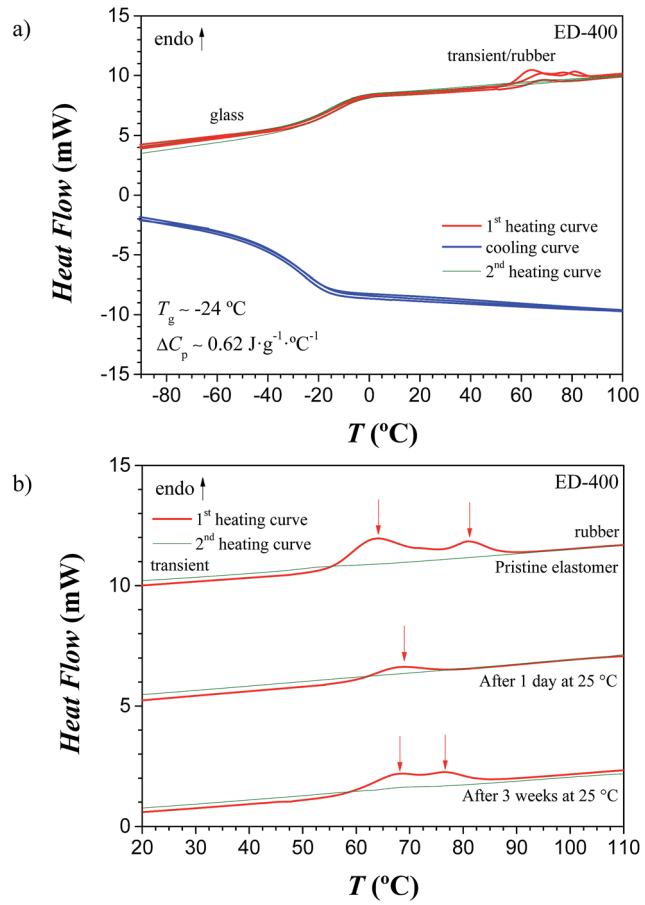

Fig. 5 (a) Different heating and cooling DSC thermographs for the elastomers ED-400 at 20 K min^{-1} showing the presence of enthalpic peaks. (b) Zoom in on the heating thermographs on the same elastomer ED-400 sample directly after the synthesis (T_{HB} ~ 64 and 81 °C, ΔH_{HB} ~ 5.2 J g^{-1}), after 1 day (T_{HB} ~68 °C, ΔH_{HB} ~1.3 J g^{-1}) and 3 weeks later (T_{HB} ~ 68 and 76 °C, ΔH_{HB} ~ 3.2 J g^{-1}). Note: the second heating curves do not show any enthalpic peak, indicating that the hydrogen bonds have not enough time to reform during the experimental time scale.

conclusion, this short segmental molecular weight polymer (DP = 6) needs very slow temperature variation in order to make visible the reversible removal of hydrogen bonds. The presence of the two DSC peaks observed when the time is enough for forming the H-bonds suggested that the formation of H-bonds is sensitive to the environment.

The presence of the transient networks can also be confirmed by FTIR experiments performed on the four elastomers at different temperatures ranging from 25 to 150 °C. The evolution of four absorption peaks was monitored from 1400 to 1800 cm^{-1}: (i) the isocyanurate peak $(NCO)_3$ from the cross-linker at $\nu_{NCO} = 1690\ cm^{-1}$; (ii) the amide I peak corresponding to the C=O stretching of the urea motives from 1630 to 1660 cm^{-1}; (iii) the amide II peak corresponding mainly to the N–H bending of the urea motives from 1505 to 1570 cm^{-1}; and (iv) the CH_2 bending at $\nu_{CH_2} = 1460\ cm^{-1}$ (Fig. ESI-2†).[53] It should be noted the reversible character of the samples after heating at 150 °C and cooling back to 25 °C, which demonstrates the stability of both the isocyanurate and urea functional groups with no dissociation or further reactions. The results show that both non-urea-related peaks have small shifts upon heating: the isocyanurate peak has an upshift of $\Delta\nu_{NCO} = +3\ cm^{-1}$, and the methylene peak has a downshift of $\Delta\nu_{CH_2} = -3\ cm^{-1}$, though we can consider them as constant peaks. The amide I peak shows an upshift and the amide II peak a downshift upon heating of the sample. Both peaks strongly depend on the chemical structure of the soft polymer backbone. The network containing the low molecular weight polymer (ED-400) or the network with non-hydrogen bonding (ESD-2001) show shifts of around $\Delta\nu = \pm 15\ cm^{-1}$, while the networks containing hydrogen bonded high molecular weight polymer (ED-2000 and ED-4000) show broader shifts of around $\Delta\nu = \pm 25\ cm^{-1}$.[54] The most relevant difference comes when comparing the peak positioning of both amide I and II at room temperature. Elastomers with a transient network (ED-400, ED-2000 and ED-4000) have the amide I peak around $\nu_{aI} = 1630\ cm^{-1}$ and the amide II peak at $\nu_{aII} = 1566\ cm^{-1}$, whereas the sample with no transient network (ESD-2001) have the peaks at $\nu_{aI} = 1640\ cm^{-1}$ and $\nu_{aII} = 1521\ cm^{-1}$, respectively, which confirms the presence of ordered hydrogen bonds for the disubstituted urea motives and disordered hydrogen bonds for the trisubstituted urea motives. All peaks at 25 °C together with the corresponding shifts upon heating the samples at 150 °C are collected in Table 1.

The presence or absence of the urea motives can be deduced from the analysis of the DSC curves of Fig. ESI-3† obtained on the four elastomers. The curves corresponding to the elastomers ED-2000 and ED-4000 (*i.e.*, the elastomers with disubstituted urea motives and long segmental molecular weight of the polymer) show a low glass transition temperature, $T_g \sim -65$ °C and −71 °C, respectively, and an endothermic peak related to the hydrogen bonding of the urea groups around $T_{HB} \sim 40$ and 60 °C, which might be associated to different nature – bidentated or monodentated – of the hydrogen bond between the urea groups. The observation of an endothermic peak for the elastomers ED-2000 and ED-4000 is consistent with the jumps observed in G'.

In contrast, the DSC curves (second and posterior heating curves) of the elastomer ED-400 (*i.e.*, the elastomer with disubstituted urea motives and short segmental molecular weight of the polymer) only show a change in the slope of the curves revealing the presence of a glass transition with a glass transition temperature $T_g \sim -24$ °C due to the reduced mobility of the short polymer leading to a greater difficulty for the urea motives to interact as explained before. Finally, the DSC curves of the elastomer ESD-2001 (*i.e.*, the elastomer with trisubstituted urea motives and long segmental molecular weight of the polymer) show a glass transition temperature at $T_g \sim -74$ °C but no endothermic peak. This is consistent with the absence of the increase observed in G' that indicates that trisubstituted urea motives cannot form hydrogen bonds. To close this section it should be noted that the DSC curves obtained by cooling do not reveal the presence of the hydrogen bonds, in contrast to the shear measurements which shows a huge increase in the G' behaviour.

Table 1 Absorption FTIR peaks at $T = 25\ ^{\circ}C$ and the corresponding shifts observed upon heating to $T = 150\ ^{\circ}C$ for the four elastomers containing diamino-terminated polyetheramine polymer

Sample	ν_{NCO} (cm^{-1})	$\Delta\nu_{NCO}$ (cm^{-1})	ν_{aI} (cm^{-1})	$\Delta\nu_{aI}$ (cm^{-1})	ν_{aII} (cm^{-1})	$\Delta\nu_{aII}$ (cm^{-1})	ν_{CH_2} (cm^{-1})	$\Delta\nu_{CH_2}$ (cm^{-1})
ED-400	1685	+3	1631	+12	1563	−15	1460	−5
ED-2000	1689	+2	1630	+26	1567	−27	1461	−4
ED-4000	1689	+2	1630	+21	1567	−31	1461	−4
ESD-2001	1691	+1	1640	+12	1521	−13	1461	−4

This is due to the difference in the cooling rate, which is slow enough ($dT/dt = 3\ K\ h^{-1}$ between two temperatures of measurement plus 1 h for taking a frequency spectrum at each temperature of measurement) for forming the hydrogen bonds in the mechanical measurements, and too fast ($dT/dt = 5\ K\ min^{-1}$) in the DSC measurements.

The number average molecular weight M_n, the segmental molecular weight M_c, the storage modulus G', the Young's modulus E, and the glass transition temperature T_g for the four elastomers containing diamino-terminated polyetheramine polymer are shown in Table 2.

Mechanical and thermodynamic behaviour of the elastomers containing triamino-terminated polyetheramines as a function of temperature

A series of four polyurea elastomers containing triamino-terminated polyetheramine (star-like polymer) was prepared by varying the molecular weight of the soft domain and the degree of substitution of the amine group. This series consists of three elastomers, ET-403, ET-3000 and ET-5000, with primary amino groups leading to disubstituted urea motives and one elastomer EST-404 with secondary amino groups forming trisubstituted urea motives. This choice allowed us to study the effect of the degree of polymerisation of the polyetheramine, the ability to form hydrogen bonds as function of the degree of substitution in the urea motive, and the presence of another crosslinker coming from the star-like architecture of the polyetheramine.

Fig. 6a shows the results obtained for the elastomer ET-403. As previously observed in the case of ED-2000, G' exhibits a sharp increase when the temperature is decreasing and a sharp decrease when the temperature is increasing. However these effects cannot be associated with the formation and melting of a transient network formed by hydrogen bonds, as in the case of ED-2000, because the sample response is under the influence of the glass transition which is very high for this compound since it occurs at around $T_g \sim +10\ ^{\circ}C$. Fig. 6a also shows that the breaking of hydrogen bonds takes place at a temperature lower than the temperature of the hydrogen bonds formation, which is contrary to the situation observed for the other elastomers, and which might be due to a coupling between the glass transition effects and the hydrogen bonds.

To clarify the behaviour observed for the elastomer ET-403, we studied the elastomer EST-404 which exhibits no hydrogen bonds. The results obtained for this elastomer, are reported on Fig. 6b. They show that G' exhibits a steep variation of nearly two orders of magnitude on a temperature range similar to the one corresponding to the increase and decrease observed for ET-403 (Fig. 6a). Given that the glass transition temperature is around $T_g \sim +29\ ^{\circ}C$, and that there are no hydrogen bonds formed due to the presence of trisubstituted urea motives, this huge variation can clearly be attributed to the dynamics of the glass transition, and the elastic plateaus observed below $T \sim +10\ ^{\circ}C$ and above 60 °C to the glassy plateau and to the permanent plateau, respectively. As the values of these plateaus are almost identical to the values found for the two plateaus of the elastomer ET-403, these latter two plateaus can therefore be attributed to the glassy and to the permanent plateau, respectively.

These results therefore lead to the conclusion that the behaviour previously observed for ET-403 results from the contributions of both the dynamics of the glass transition and of the hydrogen bonds occurring in the same temperature range. The contribution of the glass transition is more sizable than that of the hydrogen bonds, since the value of the glassy

Table 2 The number average molecular weight M_n, the segmental molecular weight M_c in the rubbery plateau (the values in parenthesis correspond to the segmental molecular weight when there is hydrogen bonding between the urea motives), the storage modulus G' and the Young's modulus E both measured at 25 °C, and the glass transition temperature T_g for the four elastomers containing diamino-terminated polyetheramine polymer[a]

Sample	M_n ($g\ mol^{-1}$)	M_c ($g\ mol^{-1}$)	$G_{cooling}'$ (Pa)	E (Pa)	T_g (°C)
ED-400	460	712[a] (460)	6.67×10^5	2.55×10^7	−24
ED-2000	2060	2312[a] (2060)	2.81×10^6	7.54×10^6	−65
ED-4000	4000	4252[a] (4000)	2.51×10^6	4.79×10^6	−71
ESD-2001	2050	2302[a]	4.31×10^5	1.18×10^6	−74

[a] Note: the segmental molecular weight M_c for these polyetheramines is the number-average molecular mass M_n plus twice the hexylisocyanate mass from the crosslinker (126 Da): [a]$M_c = M_n + 252$.

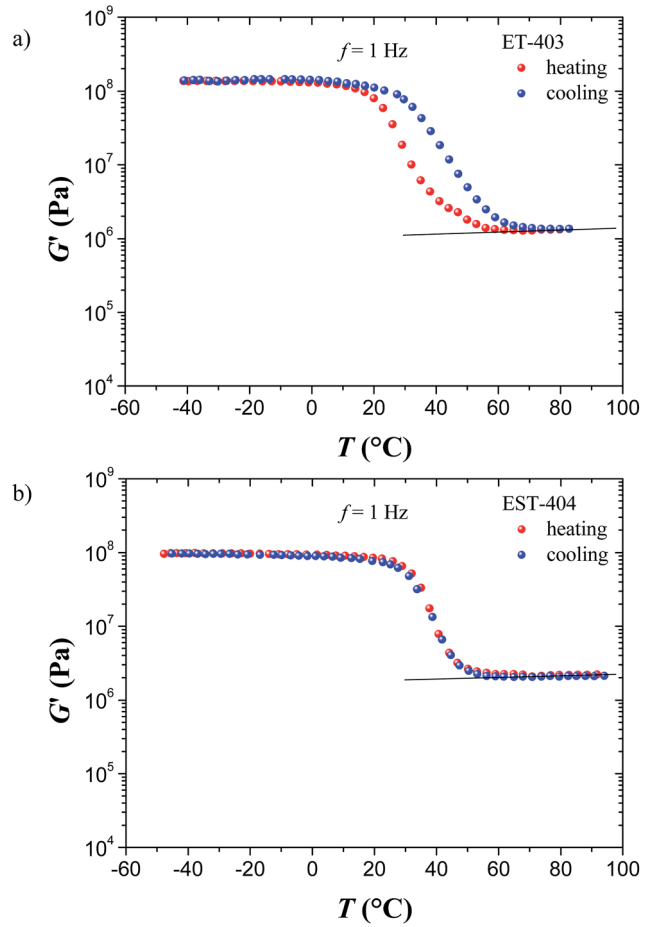

Fig. 6 Temperature dependence at $f = 1$ Hz of G' for (a) the elastomer ET-403 (primary amino-terminated polyetheramine which forms disubstituted urea groups with bidentated hydrogen bonds) at $dT/dt = 3$ K h^{-1}, and for (b) the elastomer EST-404 (secondary amino-terminated polyetheramine which forms trisubstituted urea groups without bidentated hydrogen bonds) at $dT/dt = 3$ K h^{-1}. The step variation comes from the contribution of the glass transition for EST-404, and from the simultaneous contribution of the glass transition and of the hydrogen bonds for ET-403. For both elastomers, the solid lines represent the classical k_BT behaviour.

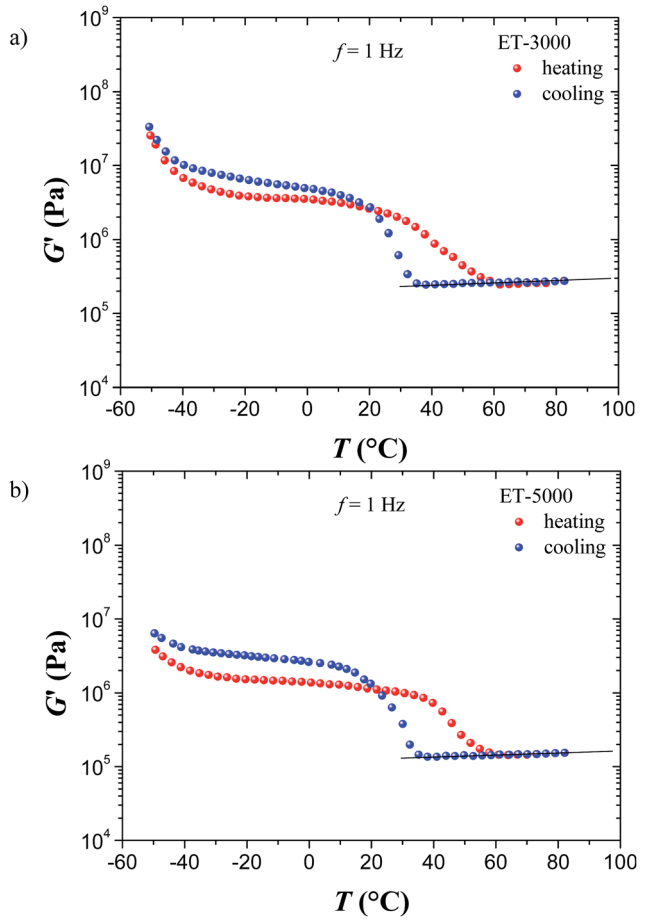

Fig. 7 Temperature dependence at $f = 1$ Hz of G' for the elastomers containing primary amino-terminated polyetheramines at $dT/dt = 3$ K h^{-1}: (a) the elastomer ET-3000, and (b) the elastomer ET-5000. The solid lines represent the classical k_BT behaviour.

plateau of ET-403 is of the same order of magnitude than the one of EST-404. The contribution of the hydrogen bonds is reflected by the thermal hysteresis observed between the heating and the cooling processes.

We consider now the elastomers ET-3000 and ET-5000, which exhibit very low glass transition temperatures, $T_g \sim -60$ °C for ET-3000 and $T_g \sim -67$ °C for ET-5000. The glass transition effects should therefore not interfere with the formation or breaking of the hydrogen bond network. Fig. 7a (ET-3000) and 7b (ET-5000), respectively, show that this is effectively the case since for both elastomers the temperature of formation of the transient network is located well above the glass transition temperature, as it is the case for the elastomers ED-2000 and ED-4000. It can also be seen that the variation of G' as a function of temperature when the glass transition is approached, is different from that of the diamino-terminated polymer-based elastomers. This difference in behaviour reflects the difference in the chemical composition and architecture (trifunctionalized *vs.* bifunctionalized polymers) of the samples.

FTIR experiments confirmed the presence or the absence of a transient network as discussed before (Fig. ESI-4†). The two elastomers containing the low molecular weight polymer (ET-403 and EST-404) show shifts of around $\Delta\nu = \pm 15$ cm^{-1} for both amide absorption bands, while the two elastomers containing the high molecular weight polymer (ET-3000 and ET-5000) show bigger shifts of around $\Delta\nu = \pm 25$ cm^{-1}. The three elastomers with the transient network (ET-403, ET-3000 and ET-5000) have the amide I peak around $\nu_{aI} = 1634$ cm^{-1} and the amide II peak at $\nu_{aII} = 1563$ cm^{-1}, whereas the elastomer with no transient network (EST-404) has the peaks located at $\nu_{aI} = 1631$ cm^{-1} and $\nu_{aII} = 1525$ cm^{-1}, respectively, differentiating the ordered disubstituted urea motives from the disordered trisubstituted urea motives. All peaks at $T = 25$ °C together with the corresponding shifts observed upon heating the elastomers to $T = 150$ °C are collected in Table 3.

Similar observations can be deduced from the analysis of the DSC curves taken for the four elastomers. Indeed, Fig. ESI-5† shows that the elastomers ET-3000 and ET-5000 with

Table 3 Absorption FTIR peaks at $T = 25$ °C and the corresponding shifts observed upon heating to $T = 150$ °C for the four elastomers containing triamino-terminated polyetheramine polymer

Sample	ν_{NCO} (cm^{-1})	$\Delta\nu_{NCO}$ (cm^{-1})	ν_{aI} (cm^{-1})	$\Delta\nu_{aI}$ (cm^{-1})	ν_{aII} (cm^{-1})	$\Delta\nu_{aII}$ (cm^{-1})	ν_{CH_2} (cm^{-1})	$\Delta\nu_{CH_2}$ (cm^{-1})
ET-403	1684	+2	1636	+10	1561	−13	1458	−3
ET-3000	1689	+2	1634	+23	1564	−23	1460	−3
ET-5000	1690	+1	1633	+21	1565	−25	1460	−3
EST-404	1685	+3	1631	+15	1525	−15	1459	−3

disubstituted urea motives and long segmental molecular weight of the polymer show a low glass transition temperature, and an endothermic peak related to the hydrogen bonding of the urea groups around $T_{HB} \sim 40$ and 60 °C, as observed previously in the case of elastomers ED-2000 and ED-4000. Fig. ESI-5† also shows that the elastomers ET-403 and EST-404 with disubstituted or trisubstituted urea motives of the polymer and short segmental molecular weight exhibit only a glass transition temperature at high temperatures, and no endothermic peak. For the elastomer EST-404 the absence of an endothermic peak is consistent with the absence of a jump in G', while for the elastomer ET-403, the situation is slightly different since this elastomer exhibits a transient network, which is not directly observed because of the proximity of the glass transition, but which is detected from the hysteresis effect between the cooling and the heating curves. As for the elastomer ED-400, mechanical experiments at very slow heating rate and up to high temperatures should allow detecting the jump in G', as observed in Fig. 3b where the transient plateau occurs below 70 °C.

The number average molecular weight M_n, the segmental molecular weight M_c, the storage modulus G', the Young's modulus E, and the glass transition temperature T_g for the four elastomers containing triamino-terminated polyetheramine polymer are shown in Table 4.

Finally, we compare the measurements of G' to the measurements of E deduced from the stress–strain experiments performed at $T = 25$ °C (Fig. 8). Since the Young's moduli E were obtained after heating the elastomers to remove all effects due to their thermal history, the comparison must be made with the values of G' determined on cooling. Owing the static character of the E measurements, this comparison also requires that the measurements of G' at $f = 1$ Hz correspond to the hydrodynamic regime. The results reported in Tables 2 and 4 show that the relationship $E = 3G'$ of the Gaussian rubber elasticity, is verified to within 10% for all the elastomers for which the G' measurements at $f = 1$ Hz belong to the hydrodynamic or almost-hydrodynamic regime. This also indicates that the G' measurements were performed at thermodynamic equilibrium. On the other hand, the relationship $E = 3G'$ does not apply for elastomers ED-400 and ET-403, for which both the hydrogen bonds and the glass transition effects contribute to G' at $T = 25$ °C, which suggests that both elastomers were not at thermal equilibrium during the G' measurements. Fig. 9 gives the plot of E *versus* G' for all the elastomers studied. The discrepancies between the E measurements and some of the previous reported results,[8] could be attributed to the sample preparation and to the thickness of the films used to perform these experiments.

We conclude this section by underlying that the segmental molecular weight – degree of polymerisation – of the networks plays a big role on the glass transition temperature and on the mechanical properties. More precisely, for each series ED or ET, reducing the polymer length between the crosslinking points increases the glass transition temperature (Fig. 10).[55–57] The presence of a soft crosslinker, as it is the case for the series ET, which acts as an impurity to the system, reduces the extrapolated glass transition temperature T_g^{∞}, as observed when the Fox–Flory empirical model is applied.[55,56] This soft crosslinker does not contribute to any extent to the shear storage modulus of the permanent network at high temperature, as observed in Fig. 11. The elastomer ESD-2001 and EST-404 – with secondary amino-terminated polyetheramine – are not following the Fox–Flory empirical model because of the absence of bidentated hydrogen bonds and the presence of bulky isopropyl groups which infer a different mobility to the segmental polymer length. The fact that the values of G' as a function of the

Table 4 The number average molecular weight M_n, the segmental molecular weight M_c in the rubbery plateau (the values in parenthesis correspond to the segmental molecular weight when there is hydrogen bonding between the urea motives), the storage modulus G' and the Young's modulus E both measured at 25 °C, and the glass transition temperature T_g for the four elastomers containing triamino-terminated polyetheramine polymer[a]

Sample	M_n (g mol^{-1})	M_c (g mol^{-1})	$G_{cooling}'$ (Pa)	E (Pa)	T_g (°C)
ET-403	486	274[a] (148)	9.76×10^7	1.39×10^8	+10
ET-3000	3180	1182[b] (1056)	1.47×10^6	4.17×10^6	−60
ET-5000	5712	2026[b] (1900)	7.77×10^5	2.25×10^6	−67
EST-404	565	301[a]	6.97×10^7	1.95×10^8	+29

[a] Note: since these polyetheramines contain a trifunctionalized crosslinker, the segmental molecular weight M_c is a third of the number-average molecular mass M_n plus the hexylisocyanate mass from the crosslinker (126 Da): [a]$M_c = (M_n - 41)/3 + 126$ and [b]$M_c = (M_n - 13)/3 + 126$.

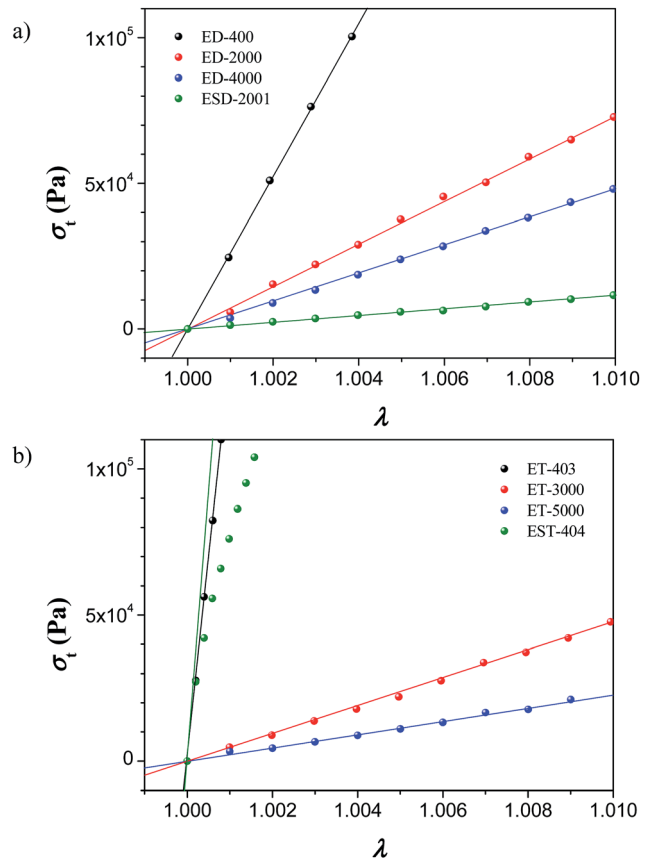

Fig. 8 Stress–strain curves at $T = 25$ °C for the elastomers ED-400, ED-2000, ED-4000 and ESD-2001 (a), and for the elastomers ET-403, ED-3000, ET-5000 and EST-404 (b). The solid straight lines are the fits of the data belonging to the purely elastic region.

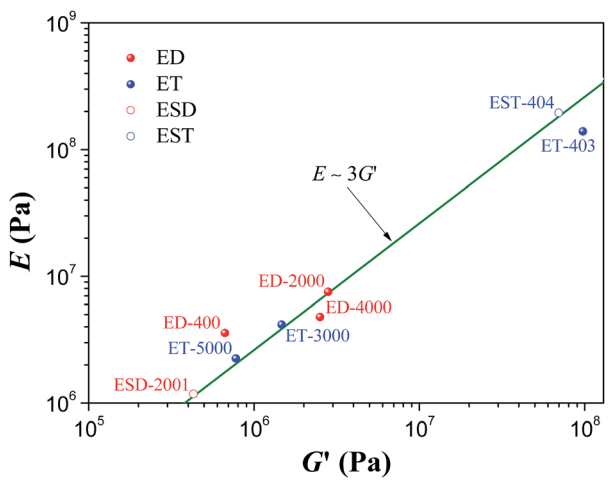

Fig. 9 *E versus G′* at $T = 25$ °C for the various elastomers studied. The *E* and *G′* measurements were taken after cooling the elastomers. The data are consistent with the relationship $E = 3G'$ represented by the solid straight line, except for elastomers ED-400 and ET-403, for which both glass transition effects and hydrogen bonds contribute to *G′* at this temperature.

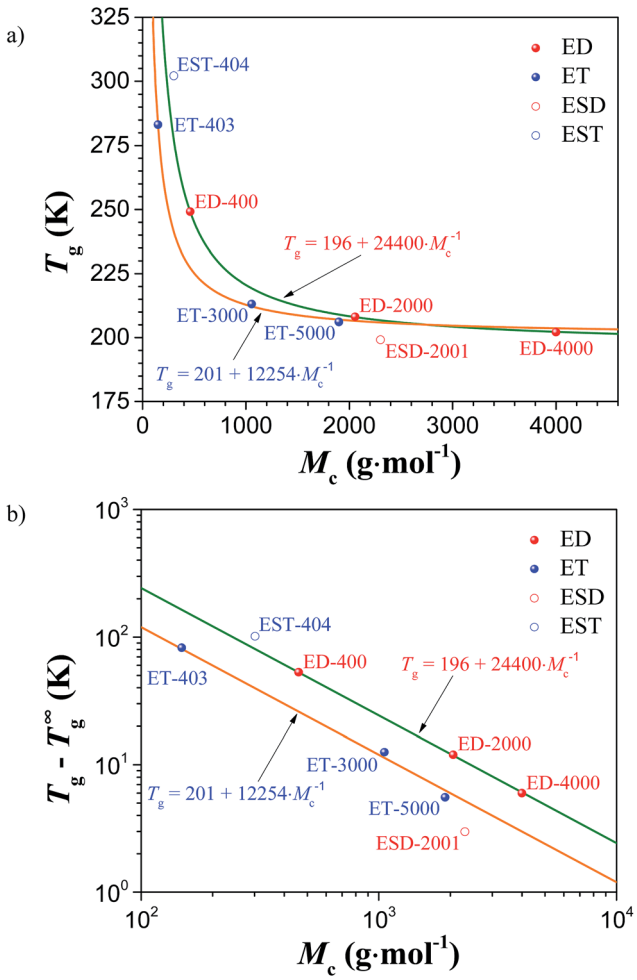

Fig. 10 (a) Linear–linear plot and (b) log–log plot for the variation of the glass transition temperature T_g as function of the segmental molecular weight M_c for the eight elastomers, showing for each series ED and ET that the short polymers raise the glass transition temperature due to the low mobility of the polymer segments between crosslinking points. T_g^{∞} is the extrapolated glass transition temperature at infinitum segmental molecular weight from the Fox–Flory empirical model. The elastomers ESD-2001 and EST-404 do not follow the Fox–Flory laws for the ED and ET series because of their different architecture.

segmental molecular weight M_c lay on a straight line for all the elastomers belonging to the ED and ET series shows the good agreement between the mechanical experiments and the chemistry of these elastomers. It also shows that the difference in the architecture of the ED and ET elastomers plays a minor role on their elasticity. In contrast, the large difference between the *G′* values of the EST-404 and ESD-2001 with respect to the corresponding hydrogen bond-containing elastomers (ET-403 and ED-2000, respectively) indicates that the architecture of the EST-404 and EST-2001 elastomers strongly differs from that of the ET-403 and ED-2000 elastomers. One possible explanation can be the presence of defects – dangling chains or longer chains – due to a mismatch in the stoichiometric ratio between the isocyanate and the amino groups, which gives an apparent segmental molecular weight bigger than the theoretical one

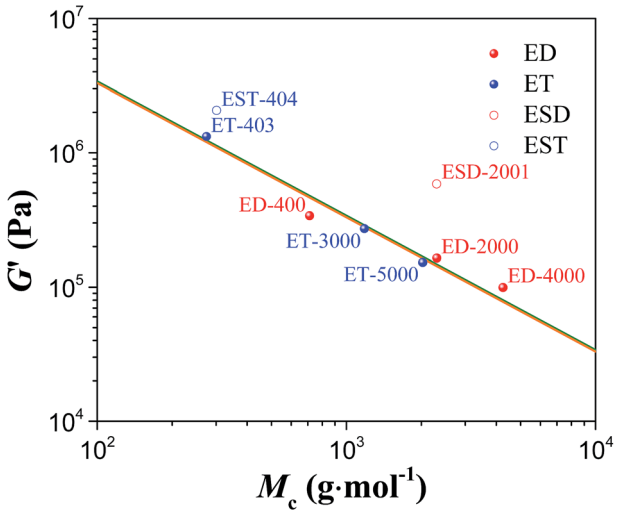

Fig. 11 log–log plot of the shear storage modulus G' as a function of the segmental molecular weight M_c for the eight elastomers at $T = 80$ °C, where the measurements correspond to the elastic plateau of the chemical network. For each series ED and ET, the data are consistent with the relationship $G' \propto M_c^{-1}$ represented by the solid straight lines. The fact that the data of the elastomers EST-404 and ESD-2001 are not on the solid straight lines associated with the ED and ET series shows that the architecture of these two elastomers strongly differs from that of the elastomers of each series.

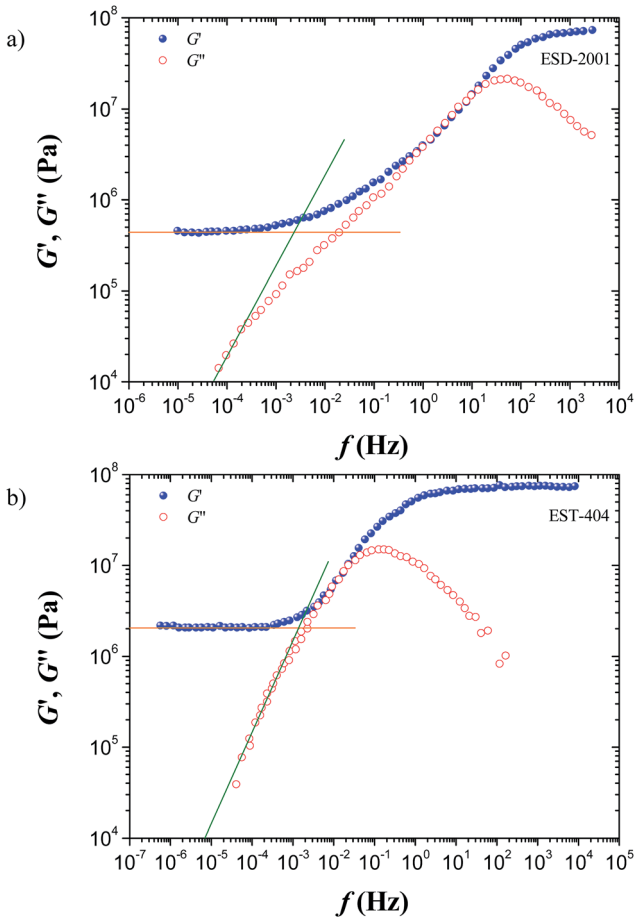

Fig. 12 (a) Master curve for the sample ESD-2001 (long secondary amino-terminated polyetheramine) showing the frequency response of the system from the hydrodynamic region up to the glassy region. The reference temperature is $T_{ref} = -45.7$ °C, and the temperature used to build the curve is $T = -3.6$ °C. (b) Master curve for the sample EST-404 (short secondary amino-terminated polyetheramine) showing the frequency response of the system from the hydrodynamic region up to the glassy region. The reference temperature is $T_{ref} = 27.5$ °C and the temperatures used to build the curve are $T = +53.1$ °C and +79.3 °C.

while keeping unchanged the relationship $E = 3G'$. This could also explain why the elastomers EST-404 and ESD-2001 do not follow the Fox–Flory law observed for the ED and ET series (Fig. 10b). Moreover, the presence of the disubstituted urea motives allow for the formation of well-ordered hydrogen bonds which lead to the formation of a transient network. This transient network vanishes upon heating the elastomers above $T \sim 60$ °C, as shown by the mechanical response of the samples and the shift of the amide I and amide II absorption peaks in the FTIR spectra (Fig. ESI-6†). Only samples with bidentated urea motives (ED-400, ED-2000, ED-4000, ET-403, ET-3000 and ET-5000) show the presence of such behaviour. The transient network cannot be mechanically detected from the G' values for ET-403 elastomer with low segmental molecular weight and ordered bidentated hydrogen bonds due to the proximity of the glass transition temperature, but from the hysteresis effect when comparing cooling and heating curves. Finally, trisubstituted urea groups show no effect in the mechanical properties of the corresponding polymer networks ESD-2001 and EST-404.

Mechanical behaviour of the various elastomers as a function of frequency

In this section, the frequency-response of the various elastomers will be presented and discussed. Firstly, we consider the elastomers that exhibit no hydrogen-bonds, *i.e.*, the elastomer ESD-2001 and EST-404 based on a diamino-terminated polymer and on a triamino-terminated polymer, respectively. Fig. 12a (ESD-2001) and 12b (EST-404) show that a master curve can be constructed for each elastomer by applying the time–temperature superposition method, which allows determining the frequency-response of each elastomer in their hydrodynamic, viscoelastic and glassy regimes. It should be noted that these master curves were obtained without making a shift along the G-axis. The differences in the hydrodynamic values of the shear modulus ($G' \sim 4 \times 10^5$ Pa for ESD-2001 compared to $G' \sim 2 \times 10^6$ Pa for EST-404), and in the width of the viscoelastic regime (ranging from $f \sim 10^{-3}$ Hz to 10^2 Hz for ESD-2001, and from 10^{-3} Hz to 10^{-1} Hz for EST-404) reflect the difference in the architectures of the elastomers (differences in the segmental molecular weight and in the nature and concentration of the crosslinkers).[8] Note that the viscoelastic behaviour is Rouse type ($G' = G''$) for both elastomers.

Secondly, we consider elastomers which exhibit a physical (transient) network due to hydrogen bonds and occurring at a temperature much higher than the glass transition temperature. These elastomers are the long segmental molecular weight elastomers ED-2000, ED-4000, ET-3000 and ET-5000,

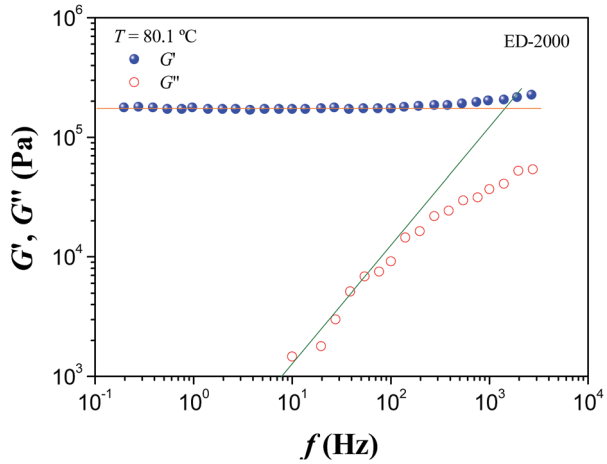

Fig. 13 Behaviour of G' and G'' as a function of frequency for the elastomer ED-2000 at a temperature located above the temperature of formation of the transient elastomer showing that the low frequency response of the material is that of a chemically crosslinked elastomer and not that of a long chain polymer.

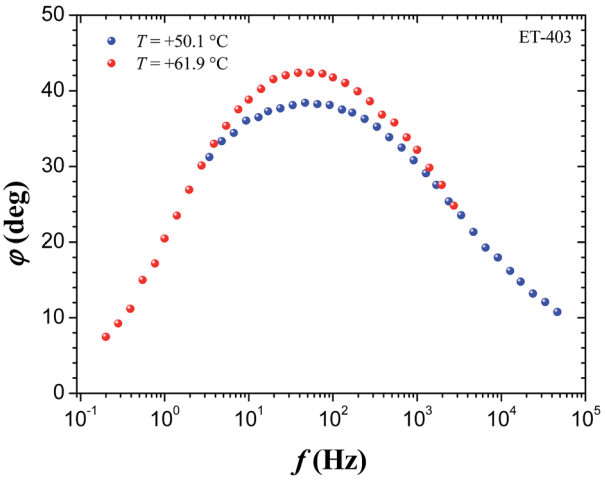

Fig. 15 Behaviour of the loss angle φ as a function of frequency for the elastomer ET-403. The temperatures of measurement are T = +50.1 °C and +61.9 °C. The last curve has been shifted along the frequency axis to show that the time–temperature superposition method does not work.

which are based on a diamino-terminated or triamino-terminated polymer.

The experiments performed as a function of frequency on these elastomers above the temperature where the transient elastomer forms show that the frequency response is composed of two regions: a low frequency region, which corresponds to the hydrodynamic behaviour for which G' is frequency independent and $G'' \propto f$, and a high frequency region characterized by a departure of G' and G'' from these laws. A typical example of the response is illustrated by Fig. 13 relative to ED-2000. The frequency-independent behavior of G' confirms that the material is an elastomer and not a relaxing liquid. Fig. 14 shows the results obtained as a function of frequency for the same elastomer at two temperatures, which, as a result of the wide frequency range given by the piezorheometer, are sufficiently close to cover the frequency response from the rubbery plateau to the glass transition.

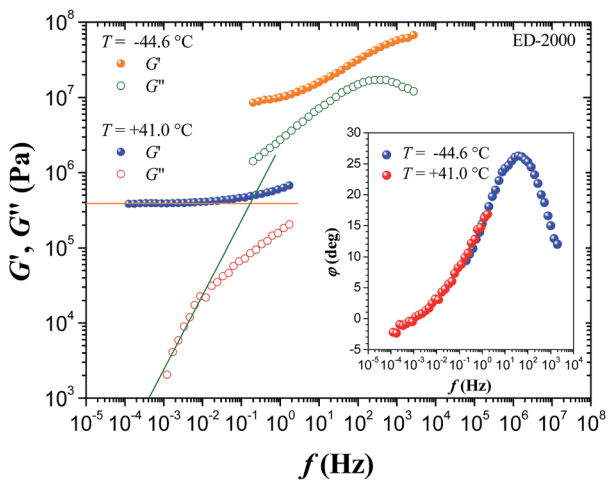

Fig. 14 Behaviour of G' and G'' as a function of the frequency for the elastomer ED-2000 showing that the time–temperature superposition method does not work. The shift factor corresponds to the one used to obtain the master curve for the loss angle φ, represented in the insert of the figure. A shift factor of 17 along the G-axis would be needed to obtain a master curve for G' and G''.

It can be seen that a single curve for the loss angle φ can be obtained by making a shift along the frequency-axis, but this shift does not allow obtaining single curves for G' and G''. This demonstrates that the time–temperature superposition method does not work for G' and G''. In contrast to the samples without hydrogen bonds, an additional shift, along the G-axis, is needed to obtain a single curve for G' and G''. Note that vertical shifts are in fact generally allowed, but these shifts must be small since they correspond to density variations.[58] The analysis of the elastomers ED-4000, ET-3000 and ET-5000 also shows that the time–temperature superposition method does not apply for these elastomers. This comes from the fact that the hydrogen-bonds and the polymer chains do not follow the same temperature dependence. As a result, the viscoelastic behaviour is clearly not of the Rouse-type, in contrast to the one for ESD-2001 and EST-404.

Finally, we consider the elastomer for which the contributions of the glass transition and of the hydrogen bonds occur in the same temperature range. This elastomer is ET-403 with short segmental molecular weight triamino-terminated polymer. Fig. 15 shows the frequency-variation of the loss angle φ for the sample ET-403 at T = +50.1 and +61.9 °C. The lack of superposition of the two curves demonstrates that the time–temperature superposition method does not work because of the simultaneous presence of the hydrogen bonds and glass transition effects.

Conclusions

We have studied the mechanical properties of a new kind of polyurea elastomers prepared by sol–gel chemistry, as a

function of the segmental molecular weight and the chemical nature of the polymer end groups. We show that their mechanical response depends on the temperature range investigated. At high temperatures, where the hydrogen bonds are not present, the response of the elastomers is the one of conventional elastomers, while at lower temperatures, when the urea motives are become hydrogen-bonded, the response of the elastomers corresponds to that of physical elastomers.

In addition to the glassy plateau, the elastomers with primary amines as terminal groups and segmental molecular weight bigger than $M_c \approx 1000$ g mol^{-1} (ED-2000, ED-4000, ET-3000 and ET-5000) show two well separated elastic plateaus respectively corresponding to the chemical and the physical components of the elastomers, while the elastomers with lower segmental molecular weight show either only the chemical plateau because the contribution of the hydrogen bonds overlaps with that of the glass transition (ET-403), or again the two plateaus (chemical and physical), but only when the heating rate is low enough for the hydrogen bonds to have time to break (ED-400). When the terminal group is a secondary amine (EST-404 and ESD-2001), which leads to the formation of trisubstituted urea motives, the corresponding elastomers show only the chemical plateau, as for the common rubber-like materials.

All elastomers from the ET series have a soft crosslinker in the chemical composition. At low temperatures, the influence of this second crosslinker has an impact on the glass transition temperature T_g, as shown by the lower value of the extrapolated glass transition temperature obtained when compared to the ED series. In contrast, at high temperatures, this soft crosslinker has almost no effect on the hydrodynamic mechanical response of the elastomers, and both ED and ET elastomers fall onto the G' *versus* M_c straight line.

For all elastomers with bidentated urea motives and segmental molecular weights higher than $M_c \approx 1000$ g mol^{-1}, the rigidity of the elastomers is reinforced by hydrogen bonds by more than one order of magnitude. These systems combine the mechanical properties of physical and chemical elastomers which form in the temperature range investigated, and can therefore be considered as selective composite materials, due to the presence of microphase separation of the hard (crosslinker) and soft (polymer chain) domains. Thus, further NMR relaxometry and Multiple Quantum NMR (MQ-NMR) experiments will be performed in order to elucidate the change in the segmental molecular weight from the transient to the purely chemical network, and the dynamical and topological influence of constraints to the polymer chains in the different polyurea elastomers.

Acknowledgements

We are grateful to Huntsman International LLC and BASF SE for kindly providing all the chemicals. We thank Dominique Collin for his friendly help during some measurements.

References

1 S. Braley, *J. Macromol. Sci., Part A: Pure Appl.Chem.*, 1970, **4**, 529.
2 P. K. Weathersby, T. Kolobow and E. W. Stool, *J. Biomed. Mater. Res.*, 1975, **9**, 561.
3 J. H. Boretos and W. S. Pierce, *Science*, 1967, **158**, 1481.
4 R. W. Hergenrother, X. H. Yut and S. L. Cooper, *Biomaterials*, 1994, **15**, 635.
5 P. Vermette, H. J. Griesser, G. Laroche and R. Guidoin, *Biomedical Applications of Polyurethanes*, Landes Bioscience, Georgetown, Texas, USA, 2001.
6 D. M. Berger and D. J. Primeaux II, Thick-Film Elastomeric Polyurethanes and Polyureas, in *The Inspection of Coatings and Linings*, The Society for Protective Coatings, Pittsburgh, 2nd edn, 2003.
7 W. D. Vilar, *Chemistry and Technology of Polyurethanes*, Vilar Polyurethanes, Rio de Janeiro, 2nd edn, 2002.
8 A. Sánchez-Ferrer, D. Rogez and P. Martinoty, *Macromol. Chem. Phys.*, 2010, **211**, 1712.
9 A. Sánchez-Ferrer, M. Reufer, R. Mezzenga, P. Schurtenberger and H. Dietsch, *Nanotechnology*, 2010, **21**, 185603.
10 A. Sánchez-Ferrer, R. Mezzenga and H. Dietsch, *Macromol. Chem. Phys.*, 2011, **212**, 627.
11 A. M. Mihut, A. Sánchez-Ferrer, J. J. Crassous, J. J. L. A. Hirschi, R. Mezzenga and H. Dietsch, *Polymer*, 2013, **54**, 4194.
12 S. Das, I. Yilgor, E. Yilgor and G. L. Wilkes, *Polymer*, 2008, **49**, 174.
13 L. Ning, W. De-Ning and Y. Sheng-Kangt, *Polymer*, 1996, **37**, 3577.
14 J. Mattia and P. Painter, *Macromolecules*, 2007, **40**, 1546.
15 R. Hill and E. E. Walker, *J. Polym. Sci.*, 1948, **3**, 609.
16 I. A. Mahammad, V. Mahadevan and M. Srinivasan, *Eur. Polym. J.*, 1989, **25**, 427.
17 X. T. Tao, T. Watanabe, D. C. Zou, S. Shimoda, H. Sato and S. Miyata, *Macromolecules*, 1995, **28**, 2637.
18 J. L. Stanford, R. H. Still and A. N. Wilkinson, *Polym. Int.*, 1996, **41**, 283.
19 S. Wataru, C. Koki and T. Naoto, *J. Polym. Sci., Part B: Polym. Phys.*, 2001, **39**, 247.
20 I. Yilgor, E. Yilgor, S. Das and G. L. Wilkes, *J. Polym. Sci., Part B: Polym. Phys.*, 2009, **47**, 471.
21 S. K. Jewrajka, J. Kang, G. Erdodi, J. P. Kennedy, E. Yilgor and I. Yilgor, *J. Polym. Sci., Part A: Polym. Chem.*, 2009, **47**, 2787.
22 R. F. Harris, M. D. Joseph, C. Davidson, C. D. Deporter and V. A. Dais, *J. Appl. Polym. Sci.*, 1990, **41**, 487.
23 L. T. J. Korley, B. D. Pate, E. L. Thomas and P. T. Hammond, *Polymer*, 2006, **47**, 3073.
24 B. Pukánszky Jr, K. Bagdi, Z. Tóvölgyi, J. Varga, L. Botz, S. Hudak, T. Dóczi and B. Pukánszky, *Eur. Polym. J.*, 2008, **44**, 2431.
25 M. A. Hood, B. Wang, J. M. Sands, J. J. L. Scala, F. L. Beyer and C. Y. Li, *Polymer*, 2010, **51**, 2191.
26 C. Z. Yang, C. Li and S. L. Cooper, *J. Polym. Sci., Part B: Polym. Phys.*, 1991, **29**, 75.
27 A. Marcos, A. Rodríguez and L. González, *J. Non-Cryst. Solids*, 1994, **172–174**, 1125.
28 N. Samcon, F. Mechin and J. P. Pascault, *J. Appl. Polym. Sci.*, 1997, **65**, 2265.

29 J. P. Sheth, E. Yilgor, B. Erenturk, H. Ozhalici, I. Yilgor and G. L. Wilkes, *Polymer*, 2005, **46**, 8185.
30 J. Yi, M. C. Boyce, G. F. Lee and E. Balizer, *Polymer*, 2006, **47**, 319.
31 S. Das, I. Yilgor, E. Yilgor, B. Inci, O. Tezgel, F. L. Beyer and G. L. Wilkes, *Polymer*, 2007, **48**, 290.
32 S. Das, D. F. Cox, G. L. Wilkes, D. B. Klinedinst, I. Yilgor, E. Yilgor and F. L. Beyer, *J. Macromol. Sci., Part B: Phys.*, 2007, **46**, 853.
33 J. L. Gallani, L. Hilliou, P. Martinoty, F. Doublet and M. Mauzac, *J. Phys. II*, 1996, **6**, 443.
34 J. Weilepp, P. Stein, N. Assfalg, H. Finkelmann, P. Martinoty and H. R. Brand, *Europhys. Lett.*, 1999, **47**, 508.
35 J. Weilepp, J. Zanna, N. Assfalg, P. Stein, L. Hilliou, M. Mauzac, H. Finkelmann, H. R. Brand and P. Martinoty, *Macromolecules*, 1999, **32**, 4566.
36 P. Stein, N. Assfalg, H. Finkelmann and P. Martinoty, *Eur. Phys. J. E*, 2001, **4**, 255.
37 J. J. Zanna, P. Stein, D. Marty, M. Mauzac and P. Martinoty, *Macromolecules*, 2003, **35**, 5459.
38 P. Martinoty, P. Stein, H. Finkelmann, H. Pleiner and H. R. Brand, *Eur. Phys. J. E*, 2004, **14**, 311.
39 D. Rogez, H. Brandt, H. Finkelmann and P. Martinoty, *Macromol. Chem. Phys.*, 2006, **207**, 735.
40 D. Rogez, G. Francius, H. Finkelmann and P. Martinoty, *Eur. Phys. J. E*, 2006, **20**, 369.
41 D. Rogez and P. Martinoty, *Eur. Phys. J. E*, 2011, **34**, 69.
42 D. Rogez, F. Brömmel, H. Finkelmann and P. Martinoty, *Macromol. Chem. Phys.*, 2011, **212**, 2667.
43 P. Martinoty, L. Hilliou, M. Mauzac, L. Benguigui and D. Collin, *Macromolecules*, 1999, **32**, 1746.
44 D. Collin and P. Martinoty, *Phys. A*, 2003, **320**, 235.
45 D. Collin and P. Martinoty, *Eur. Phys. J. E*, 2006, **19**, 87.
46 O. Pozo, D. Collin, H. Finkelmann, D. Rogez and P. Martinoty, *Phys. Rev. E: Stat., Nonlinear, Soft Matter Phys.*, 2009, **80**, 031801.
47 D. Collin, G. K. Auernhammer, O. Gavat, P. Martinoty and H. R. Brand, *Macromol. Rapid Commun.*, 2003, **24**, 737.
48 G. K. Auernhammer, D. Collin and P. Martinoty, *J. Chem. Phys.*, 2006, **124**, 204907.
49 D. Collin, P. Lavalle, J. Méndez-García, J. C. Voegel, P. Schaaf and P. Martinoty, *Macromolecules*, 2004, **37**, 10195.
50 A. Fuith, M. Reinecker, A. Sánchez-Ferrer, R. Mezzenga, A. Mrzel, M. Knite, I. Aulika, M. Dunce and W. Schranz, *Sens. Transducers J.*, 2011, **12**, 71.
51 M. Reinecker, A. Fuith, V. Soprunyuk, A. Sánchez-Ferrer, A. Mrzel, R. Torre and W. Schranz, *Phys. Status Solidi A*, 2013, **11**, 2348.
52 M. Reinecker, V. Soprunyuk, M. Fally, A. Sánchez-Ferrer and W. Schranz, *Soft Matter*, 2014, **10**, 5729–5738.
53 E. Yilgor, E. Burgaz, E. Yurtsever and I. Yilgor, *Polymer*, 2000, **41**, 849.
54 N. S. Myshakina, Z. Ahmed and S. A. Asher, *J. Phys. Chem. B*, 2008, **112**, 11873.
55 T. G. Fox and P. J. Flory, *J. Appl. Phys.*, 1950, **21**, 581.
56 T. G. Fox and P. J. Flory, *J. Polym. Sci.*, 1954, **14**, 315.
57 T. G. Fox and S. Loshaek, *J. Polym. Sci.*, 1955, **15**, 371.
58 J. D. Ferry, *Visco-Elastic Properties of Polymers*, Wiley, New York, 2nd edn, 1970.